Received: 14 May 2021 | Revised: 10 February 2023 | Accepted: 10 February 2023

DOI: 10.1111/ejn.15934

RESEARCH REPORT

EJN European Journal of Neuroscience FENS WILEY

Neural tracking of visual periodic motion

Manuel Varlet[1,2] | **Sylvie Nozaradan**[3] | **Richard C. Schmidt**[4] | **Peter E. Keller**[1,5]

[1]The MARCS Institute for Brain, Behaviour and Development, Western Sydney University, Penrith, Australia

[2]School of Psychology, Western Sydney University, Penrith, Australia

[3]Institute of Neuroscience (IONS), Université catholique de Louvain (UCL), Brussels, Belgium

[4]Department of Psychology, College of the Holy Cross, Worcester, Massachusetts, USA

[5]Center for Music in the Brain, Department of Clinical Medicine, Aarhus University & The Royal Academy of Music Aarhus/Aalborg, Aarhus, Denmark

Correspondence
Manuel Varlet, MARCS Institute for Brain, Behaviour and Development, Western Sydney University, Locked Bag 1797, Penrith NSW 2751, Australia.
Email: m.varlet@westernsydney.edu.au

Funding information
Australian Research Council, Grant/Award Number: DP170104322

Edited by: Guillaume Rousselet

Abstract

Periodicity is a fundamental property of biological systems, including human movement systems. Periodic movements support displacements of the body in the environment as well as interactions and communication between individuals. Here, we use electroencephalography (EEG) to investigate the neural tracking of visual periodic motion, and more specifically, the relevance of spatiotemporal information contained at and between their turning points. We compared EEG responses to visual sinusoidal oscillations versus nonlinear Rayleigh oscillations, which are both typical of human movements. These oscillations contain the same spatiotemporal information at their turning points but differ between turning points, with Rayleigh oscillations having an earlier peak velocity, shown to increase an individual's capacity to produce accurately synchronized movements. EEG analyses highlighted the relevance of spatiotemporal information between the turning points by showing that the brain precisely tracks subtle differences in velocity profiles, as indicated by earlier EEG responses for Rayleigh oscillations. The results suggest that the brain is particularly responsive to velocity peaks in visual periodic motion, supporting their role in conveying behaviorally relevant timing information at a neurophysiological level. The results also suggest key functions of neural oscillations in the Alpha and Beta frequency bands, particularly in the right hemisphere. Together, these findings provide insights into the neural mechanisms underpinning the processing of visual periodic motion and the critical role of velocity peaks in enabling proficient visuomotor synchronization.

KEYWORDS
electroencephalography, motion perception, neural oscillations, nonlinear movement kinematics, sensorimotor synchronization, velocity profile

1 | INTRODUCTION

Periodicity is a fundamental property of biological systems, including human movement systems. Periodic

Abbreviations: ANOVA, analysis of variance; EEG, electroencephalography; FFT, fast Fourier transform; MEG, magnetoencephalography; MT/V5, middle temporal visual area..

movements are ubiquitous in daily human activities. They support the displacement of bodies in the environment (e.g., locomotion) and interaction and communication among individuals (Coey et al., 2012; Kelso, 1995; MacRitchie et al., 2017; Schmidt & Richardson, 2008). Humans have evolved not only to have strong capacities for the production of periodic movements but also for their perception (Calvo-Merino et al., 2004; Press et al., 2005, 2011; Varlet, Novembre, & Keller, 2017; Wilson et al., 2005). However, how the brain extracts and processes behaviorally relevant timing information from observed periodic motion, allowing humans to proficiently interact with their environment and each other, remains unclear. To address this question we employ here electroencephalography (EEG) to investigate the processes underlying the neural tracking of periodic motion during passive observation, and more specifically, the role of velocity peaks in observed motion.

Numerous studies have investigated how humans extract timing information from visual periodic motion to proficiently synchronize their actions (Hajnal et al., 2009; Luck & Sloboda, 2009; Roerdink et al., 2005; Snapp-Childs et al., 2011; Su, 2016; Varlet et al., 2015; Wilson et al., 2005). Some of these studies have suggested that behaviorally relevant timing information for optimal movement synchronization is contained at the turning points of visual periodic motion. Hajnal and colleagues investigated participants' movement synchronization with a stimulus oscillating horizontally on a screen while occluding different sections of the stimulus trajectory (Hajnal et al., 2009). The results revealed that synchronization performance was degraded when turning points were occluded, whereas the occlusion of the stimulus trajectory between the turning points had negligible effects, supporting the hypothesis that critical timing cues are contained at the turning points of visual periodic motion. The superiority of turning points over the rest of the motion trajectory has also been suggested by previous research that examined eye movements during visuomotor synchronization tasks (Roerdink et al., 2005, 2008). This research showed that participants' eyes were preferentially fixated on the turning points of the stimulus oscillations. Together, these results support the hypothesis that the turning points contain relevant spatiotemporal information, which has been suggested to be due to the lower velocity at this part of the movement trajectory facilitating its extraction and processing (Bingham, 2004; Bingham et al., 2001; Hajnal et al., 2009; Wilson et al., 2005).

On the other hand, there is also research suggesting that turning points in visual periodic motion might not be the most relevant source of spatiotemporal information (Hove et al., 2010; Luck & Sloboda, 2009; Su, 2016; Varlet et al., 2015; Zelic et al., 2018). Studies have compared visuomotor synchronization with visual stimuli that either continuously oscillated between left and right turning points on a screen or only flashed at the turning points. Spatiotemporal information at the turning points was the same in both conditions, but the results indicated that synchronization performance was significantly improved with continuously oscillating stimuli (Hove et al., 2010; Zelic et al., 2018). Interestingly, there is also research showing that an individual's movement is influenced not only by the presence of the continuous flow of information between the turning points but also by the nature of the motion trajectory between the turning points. Relevant findings come from previous studies that investigated the influence of different trajectories in visual periodic motion, including human vs. nonhuman trajectories, on an observer's movement (Brass et al., 2000; Kilner et al., 2003; Varlet et al., 2014).

These studies suggested an influential role of peak velocity in visual periodic motion. Simple oscillating dots on a monitor were found to have stronger effects on the movement responses of an observer when they had velocity profiles with a salient peak (Kilner et al., 2003; 2007). The observation of an oscillating stimulus with a sinusoidal velocity profile that is typical of human periodic movements has greater influence on produced movements than a stimulus with a nonbiological constant velocity profile without a peak (Kilner et al., 2003, 2007). It has also been shown in visuomotor synchronization tasks that a nonlinear Rayleigh velocity profile, which is also typical of human movements but characterized by an earlier velocity peak than in a sinusoidal velocity profile, can further increase stimulus effects on an observer's movements (Varlet et al., 2014; Varlet, Schmidt, & Richardson, 2017; Zelic et al., 2016). Movements are synchronized with less variability and more anticipation of stimuli with a Rayleigh velocity profile compared to those with a sinusoidal velocity profile, suggesting a relevant role of velocity peaks.

It has been argued that the velocity peak in visual periodic motion contains critical timing information (Gu et al., 2019; Hove et al., 2013; Iversen et al., 2015) and that an earlier peak makes it possible for the brain to process this information sooner and more accurately. This would help an individual to make better movement adjustments that are continuously needed in synchronization tasks for optimal performance (Repp & Su, 2013; Varlet et al., 2014; Varlet, Schmidt, & Richardson, 2017; Zelic et al., 2016). The acceleration profile of visual periodic motion has also been suggested as a potential candidate in providing critical timing cues, although disentangling the respective contribution of velocity and acceleration profiles remains challenging, as they are

tightly linked (Luck & Sloboda, 2008, 2009). Irrespective of the exact role of the velocity and acceleration profiles, these findings contrast with the hypothesis that critical timing information in visual periodic motion would be restricted to spatiotemporal properties at turning points. They suggest that the brain is especially responsive to physical properties of visual periodic motion between the turning points.

Recent studies have shown that neuroimaging techniques might offer a particularly promising avenue to explore the spatiotemporal properties of visual periodic motion that are preferentially processed by the brain and used to produce synchronized movements. Indeed, there is growing evidence in the context of auditory–motor synchronization showing that the amplitude of the neural response at the frequency of periodic stimuli measured with EEG during passive listening can predict an individual's capacity to synchronize proficiently with these stimuli (Bouvet et al., 2020; Lenc et al., 2019; Nozaradan et al., 2016). It has been shown that larger EEG responses correlate with better movement synchronization across conditions and participants. Although there is still a limited understanding of how the brain processes physical properties of visual periodic motion and extracts relevant timing information, previous work from Press et al. (2011) supports the hypothesis that timing information extracted by the brain is not restricted to the turning points. Using magnetoencephalographic recordings, this study showed larger neural responses during the observation of motion with a sinusoidal velocity profile compared to a constant velocity profile. It was also reported that 20 Hz Beta-band neural oscillations, which have been linked to sensorimotor and timing mechanisms (Avanzini et al., 2012; Fujioka et al., 2012; Hari et al., 1998; Kilner et al., 2009), exhibited maximum amplitude near the velocity peak of the visual motion. These results support the possibility that the brain might be particularly sensitive to the velocity peak in visual periodic motion and that Beta-band amplitude modulations might have an important function in processing related motion information.

The current study aims to better understand how the human brain processes visual periodic motion. We compared EEG responses to sinusoidal and nonlinear Rayleigh periodic motion during passive observation to determine to what extent dynamic modulations in brain activity induced by visual periodic motion originate from the processing of spatiotemporal information contained at the turning points or between the turning points. Finding different EEG responses due to subtle variations in the velocity profiles of sinusoidal and nonlinear Rayleigh stimuli would confirm at a neurophysiological level the relevance of spatiotemporal information between the turning points and more specifically of the peak velocity. Indeed, because the stimuli were presented at the same frequency and amplitude and, thus, contained the same spatiotemporal information at the turning points, differences between the two stimuli in EEG recordings

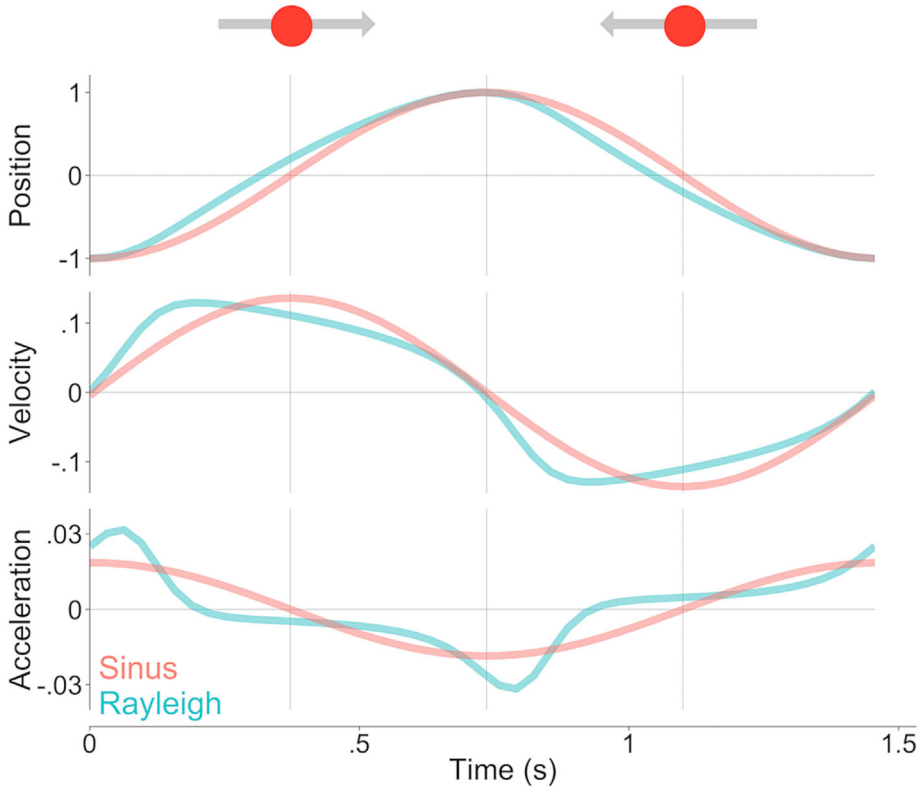

FIGURE 1 Position, velocity and acceleration profiles for one motion cycle of the visual stimuli based on Sinus (sinusoidal) and Rayleigh oscillations.

would necessarily be due to the processing of spatiotemporal information (i.e., physical properties) between the turning points.

It was first hypothesized that larger amplitude in brain activity at the stimulus frequency would occur with Rayleigh stimuli, providing a neurophysiological basis for the superior motor synchronization and temporal anticipation previously reported. This hypothesis is in line with previous studies that showed positive correlation between the amplitude of EEG response at the stimulus frequency and an individual's capacity to synchronize with the stimulus (Bouvet et al., 2020; Lenc et al., 2019; Nozaradan et al., 2016). Furthermore, we hypothesized that earlier brain response within the stimulus cycles would occur with Rayleigh oscillations, which could also explain the superior motor synchronization previously reported by leaving more time for processing the information and adequately adjusting the movement produced. This would support the relevance of the peak velocity in conveying critical timing information because it occurs earlier for Rayleigh than sinusoidal oscillations, as depicted in Figure 1. Interestingly, it can be noted that the peak acceleration actually occurs later within stimulus cycles for Rayleigh than sinusoidal oscillations (see Figure 1), providing a means for disentangling the respective contribution of velocity and acceleration profiles.

Frequency-domain and time-domain analyses were used to compare the amplitude and timing of the EEG responses induced by visual periodic motion. Frequency-domain analyses examined the amplitude and phase in the EEG activity at the stimulus frequency and its harmonics, which was the same for both Sinus (sinusoidal) and Rayleigh stimuli. Both frequency-domain and time-domain analyses examined the amplitude and timing of the EEG modulations at the stimulus frequency in broadband signals and also in the amplitude of Theta (4–8 Hz), Alpha (8–12 Hz), Beta (12–40 Hz) and Gamma (40–100 Hz) frequency-band neural oscillations to investigate their contribution to the processing of visual periodic motion. In line with previous research (e.g., Press et al., 2011), we hypothesized that modulations in the amplitude of Beta band oscillations would be implicated in the processing of visual periodic motion and the tracking of velocity variations within and across observed motions.

2 | METHODS

2.1 | Participants

Fifteen students from Western Sydney University volunteered to participate in the experiment (10 females and five males aged from 21 to 33 years; $M = 26.67$, $SD = 3.94$). The sample size was chosen according to effect sizes reported in Lenc et al. (2018) and Nozaradan et al. (2016), which used EEG frequency tagging while manipulating physical features of auditory rhythms. These studies reported large effect sizes while manipulating the timing of the acoustic rhythms (isochronous vs. syncopated; $\eta^2 = .68$) and the frequency of the sounds (low-pitched vs. high-pitched; $d > .98$). An apriori power analysis in G*power 3 (Faul et al., 2007) based on paired *t*-tests to compare amplitude and phase across stimuli indicated a required sample size of 15 participants to detect large effect sizes ($d = .8$) with at least 80% statistical power. All participants who self-reported normal or corrected-to-normal vision were right-handed and provided written informed consent prior to the experiment, which was approved by Western Sydney University Ethics Committee.

2.2 | Visual stimuli and experimental design

Visual stimuli were presented on a Samsung SyncMaster 740 N 17-in. monitor (resolution 1280 × 1024 pixels; refresh rate 60 Hz; Samsung SyncMaster, Samsung Electronics, Seoul, South Korea) 60 cm away in front of the participant seated on a chair. The visual display consisted of a red dot with a diameter of 2 cm (≈2° visual angle) oscillating horizontally on a black background at the height of the participant's eyes with an amplitude of 30 cm, which corresponded to a visual angle of approximately 28°. The frequency of the stimulus movement oscillations was .6522 Hz, which was in the range of frequencies used in previous studies that found enhanced movement synchronization and anticipation, and was adapted to the refresh rate of the monitor (one full cycle equaled 92 frames; Varlet et al., 2014; Zelic et al., 2016).

The stimulus oscillated between the right and left turning points on the screen either with a perfectly harmonic sinusoidal (i.e., Sinus) velocity profile or a Rayleigh velocity profile. The Rayleigh velocity profile was generated using the following nonlinear oscillator equation:

$$\ddot{x} - \varepsilon\left(1 - \dot{x}^2\right)\dot{x} + x = 0,$$

where x represents the position of the oscillator and the dot notation represents derivative with respect to time. $\varepsilon = 8.2$ was used in order to produce Rayleigh motion oscillations similar to previous studies with moderate deviations from perfect sinusoidal motion, thus matching the magnitude of deviations generally found in human

periodic movements (Beek et al., 1995; Varlet et al., 2014; Zelic et al., 2016). The time series were then normalized to have the same motion amplitude for all stimuli (i.e., 30 cm).

In all conditions, a fixation cross was displayed on top of the oscillating dot at the center of the screen on which letters flashed at random time intervals. The letters were used for a letter detection task in order to make sure that the participant kept focusing on the visual displays with the eyes fixated at the center of the screen throughout the trials (Schmidt et al., 2007; Varlet et al., 2014; Varlet, Novembre, & Keller, 2017). The participant was asked to keep the eyes fixated on the cross and to remember the last letter that appeared on the screen. The participant was required to report it aloud at the end of the trial under the monitoring of the experimenter. In each trial, at least one letter randomly occurred for 200 ms, and in some trials, a second letter randomly occurred in the last 10 s to ensure that the participant paid attention to the visual displays until the end. The experimenter continuously monitored that the participant adequately performed the letter detection task. All participants adequately performed the task, but the data were not recorded.

Six trials of 35 s for each of the two kinematic conditions—Sinus and Rayleigh—were presented. Additional control trials without the oscillating dot and velocity peaks were also presented but not analyzed as it is beyond the scope of this article. The total duration of the experiment was therefore about 60 min, including EEG preparation and breaks.

2.3 | EEG recording

EEG signals were recorded at a sampling rate of 2048 Hz using a Biosemi Active-Two system (Biosemi, Amsterdam, Netherlands) with 64 Ag–AgCl electrodes

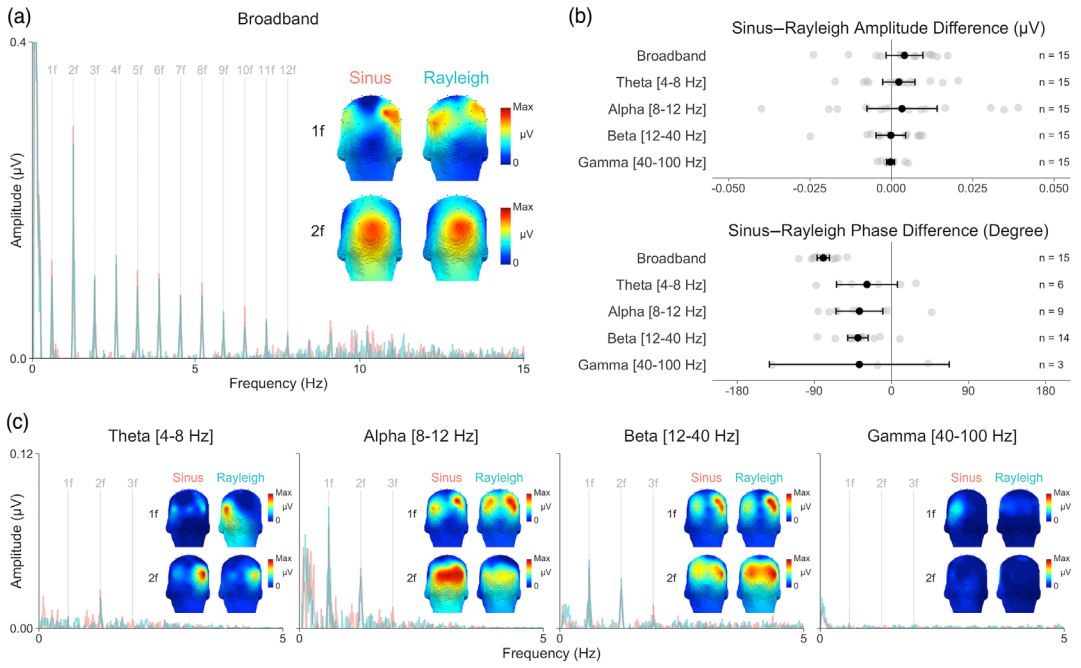

FIGURE 2 Electroencephalography (EEG) frequency-domain amplitude spectra (with baseline subtracted) averaged across selected parieto-occipital electrodes for broadband (a), Theta [4–8 Hz], Alpha [8–12 Hz], Beta [12–40 Hz] and Gamma [40–100 Hz] frequency bands (c) for Sinus and Rayleigh kinematics, with the corresponding grand-averaged topographies at the stimulus fundamental frequency (1f = .65 Hz) and first harmonic (2f = 1.3 Hz). Grand-averaged topographies in panels (a) and (c) are presented from a posterior view to show EEG activity over visual regions. Frequency-domain amplitude spectra in panel (c) for Theta [4–8 Hz], Alpha [8–12 Hz], Beta [12–40 Hz] and Gamma [40–100 Hz] were computed on the envelope of EEG signals in these frequency bands using the Hilbert transform. Panel (b) represents the differences between the Sinus and Rayleigh kinematics for the amplitude and phase of EEG responses. These amplitude and phase differences include all participants and the fundamental frequency and first 11 harmonics (1f–12f) for broadband responses. For Theta, Alpha, Beta and Gamma, the amplitude differences include all participants and the fundamental and first two harmonics (1f–3f). The phase differences for Theta, Alpha, Beta and Gamma include only participants and responses with significant amplitude (signal amplitude > noise background) within the fundamental and first two harmonics (1f–3f) to avoid the inclusion of random phase values and invalid results. Negative values indicated earlier EEG responses to the Rayleigh stimulus than the Sinus stimulus whereas positive values indicated the opposite (see Materials and Methods for further details). Error bars represent 1 × 95% CI of the mean.

placed over the scalp according to the international 10/20 system. All electrodes were referenced to the common mode sense (CMS), and their magnitude was kept below 50 μV. Four additional electrodes placed above and below the right eye and the external corner of the left and right eyes were used to record ocular movements and eye blinks.

2.4 | EEG preprocessing

EEG analyses were conducted in MATLAB (The Mathworks, Inc.) with the Fieldtrip toolbox (Oostenveld et al., 2011). Topographies were made using Letswave6 (Mouraux & Iannetti, 2008) (www.letswave.org), with the posterior view of the 3D head shape presented in the figures to facilitate visualization of EEG activity over visual regions.

EEG data were first high-pass filtered using a fourth-order Butterworth filter with a cut-off frequency of .1 Hz and downsampled to 600 Hz. Data were then segmented in 33.73 s trials containing the last 22 stimulus cycles presented. Electrodes containing excessive artifacts or noise were then interpolated with the neighboring electrodes (i.e., an average of 1 interpolated electrode per participant and never more than 3). An independent components analysis (FastICA), as implemented in Fieldtrip, was then used to remove blink artefacts. Based on the visual inspection of the topography and time-course, one single component corresponding to the blinks was removed per participant. Visual inspection of the topography and time-course did not reveal components corresponding to lateralized eye movements, indicating that participants adequately kept their eyes on the fixation cross. EEG data were then re-referenced to the average of all scalp electrodes.

To examine the changes in the magnitude of neural oscillations within different frequency bands, a fourth-order band-pass Butterworth filter was used to keep signals within the Theta (4–8 Hz), Alpha (8–12 Hz), Beta (12–40 Hz) and Gamma (40–100 Hz) bands (Bourguignon et al., 2017; Colon et al., 2017). Instantaneous amplitude of the neural oscillations in these frequency bands for each EEG electrode and trial was then extracted by computing the envelope of the signals using a Hilbert transform (Bourguignon et al., 2017; Colon et al., 2017). Computing the envelope of the signal in a particular frequency band using a Hilbert transform is an alternative to Fast Fourier Transformation (FFT)- or wavelet-based time-frequency analyses (Pikovsky et al., 2003). The Hilbert transform has the advantage of providing an instantaneous estimate of the amplitude of neural oscillations at the original sampling rate. This procedure resulted in five datasets—broadband (.1 Hz high pass filtered), Theta, Alpha, Beta and Gamma. For each of the five datasets, the six trials for each stimulus kinematics were then averaged together and kept for further frequency-domain and time-domain analyses to examine differences in amplitude and phase in the EEG tracking of the Sinus and Rayleigh kinematics.

2.5 | EEG frequency-domain responses

For the EEG frequency-domain responses, we used an FFT on these five datasets to compute the amplitude spectra up to 50 Hz with a frequency resolution of .0296 Hz (i.e., 1/33.73). In order to examine the occurrence of significant EEG responses at the stimulus fundamental frequency (i.e., .6522 Hz) and its harmonics, we pooled together EEG electrodes in parieto-occipital regions (P7, PO7, P5, P3, PO3, O1, Oz, POz, Pz, O2, PO4, P4, P6, PO8 and P8) that showed clear visual responses as seen in Figure 2 and in accordance with previous research (Jacques et al., 2016; Quek et al., 2018). We then computed the Z-scores at each frequency bin as the difference in amplitude between that frequency bin and the mean of the 20 neighbouring frequency bins (excluding the two immediately adjacent frequency bins), divided by the standard deviation of those 20 neighbouring bins. Z-scores were computed at the group level by taking the amplitude spectra averaged across all participants and the two stimulus conditions and at the individual level by taking the amplitude spectra averaged across the two stimulus conditions. EEG responses at the frequency bins corresponding to the stimulus fundamental frequency and its harmonics were considered to be significant at the group level and individual level when the Z-score value was greater than 1.96 ($p < .05$, one-tailed), in line with previous studies that used frequency-tagging techniques (Jacques et al., 2016; Quek et al., 2018; Varlet et al., 2020). Significant Z-score values indicate signal amplitudes significantly larger than the noise background. Including higher harmonics is important because they capture deviations from a perfectly sinusoidal waveform at the stimulus frequency. However, modulations at the stimulus frequency in the amplitude of faster neural oscillations are more directly captured by the envelope of the EEG signal filtered in the frequency bands of interest.

To examine differences in amplitude in the EEG responses to Sinus and Rayleigh stimulus and control for the effect of background noise, we subtracted at each frequency bin of the amplitude spectra of each participant, electrode and kinematic condition the average amplitude of the 20 neighboring frequency bins excluding the two immediately adjacent frequency bins (Lenc et al., 2018; Varlet et al., 2020). This baseline correction procedure is important because it controls for changes of amplitude in

the frequency bins of interest (i.e., .6522 Hz and its harmonics), which might be due to other factors than those manipulated, such as background noise and muscular artifacts. Such irregularities affect amplitude spectra over a large range of frequency bins around those of interest and hence are removed when subtracting adjacent frequency bins. Grand-average amplitude spectra with baseline subtraction averaged across selected parieto-occipital electrodes (P7, PO7, P5, P3, PO3, O1, Oz, POz, Pz, O2, PO4, P4, P6, PO8 and P8) for the five datasets and the two kinematic conditions are presented in Figure 2.

Amplitude data for the five datasets at the frequency bins that showed significant responses were submitted to three-way repeated-measures analyses of variance (ANOVAs) with the factors Kinematic (Sinus and Rayleigh), Electrode (left, central and right) and Harmonic (significant frequency bins). The factor Electrode was included to examine differences between left (P7, PO7, P5, P3, PO3 and O1), central (Oz, POz and Pz) and right (O2, PO4, P4, P6, PO8 and P8) parieto-occipital regions that showed different responses for the different frequency bins, as seen on the topographical maps in Figure 2. Figure 2b represents, for the different datasets, amplitude differences between the two kinematic conditions computed as Sinus amplitude minus Rayleigh amplitude averaged across all selected parieto-occipital electrodes and frequency bins. Negative values indicated larger EEG responses to the Rayleigh stimulus than the Sinus stimulus whereas positive values indicated the opposite. One-sample *t*-tests were used to test significant differences from 0 for the five datasets.

To examine differences in phase in the EEG responses to Sinus and Rayleigh stimulus, we extracted the phase in the selected parieto-occipital electrodes (P7, PO7, P5, P3, PO3, O1, Oz, POz, Pz, O2, PO4, P4, P6, PO8 and P8). Only participants and frequency bins with significant amplitude, as determined with the Z-scores (signal amplitude > background noise), were selected for this phase analysis to avoid the inclusion of random values. Non-significant frequency bins have amplitude values close to 0 and thus have negligible influence on amplitude analyses. However, nonsignificant frequency bins have random phase values between −180 and 180, which would strongly bias phase analyses. It is therefore critical for phase analyses to include only participants and frequency bins in which signal amplitude exceeds the background noise. Conducting phase analyses with the values from all participants and frequency bins despite the absence of significant amplitude would lead to invalid results. For each participant who exhibited a significant response, we computed the phase difference between the two kinematic conditions as Sinus phase minus Rayleigh phase for all selected electrodes. Negative values indicated earlier EEG responses to the Rayleigh stimulus than the Sinus stimulus whereas positive values indicated the opposite. For each dataset, all phase difference values were then averaged across electrodes and frequency bins to obtain a single value for each participant who exhibited a significant response presented in Figure 2b. The averaging was done using circular statistics to take into account the cyclic nature of phase values (Batschelet, 1981; Pikovsky et al., 2003). One-sample *t*-tests were used to test significant differences from 0 for the five datasets.

2.6 | EEG time-domain responses

For the analysis of EEG time-domain responses, we averaged together the EEG data of the last 22 stimulus cycles for each of the five datasets. The broadband (.1 Hz high pass filtered) dataset was further filtered before averaging the cycles using a fourth-order Butterworth band-pass filter with .3 and 30 Hz cut-off frequencies to remove slow trends and higher frequency noise (and fast modulations of small magnitude) to improve the visualization of these time-domain responses in line with previous research (Jacques & Rossion, 2007; Nozaradan et al., 2018; Quek et al., 2018). To identify significant differences between the EEG responses to Sinus and Rayleigh stimulus while controlling for multiple comparisons, we used cluster-based permutation analyses (Oostenveld et al., 2011). We ran point-by-point paired-sample *t*-tests to compare the two responses. Then, we determined clusters of adjacent time points above the critical *t*-value for a parametric two-sided test and the magnitude of each cluster by computing the sum of the absolute *t*-values constituting each cluster. We used 1000 random permutations of each participant's responses to obtain a reference distribution of maximum cluster magnitude. The proportion of random partitions that resulted in a larger cluster-level statistic than the observed one (*p* value) was calculated. Clusters in observed data were considered as significant if their magnitude exceeded the threshold of the 95th percentile of the permutation distribution. Grand-average time-domain responses to Sinus and Rayleigh stimulus for the five datasets and for left (P7, PO7, P5, P3, PO3 and O1), central (Oz, POz and Pz) and right (O2, PO4, P4, P6, PO8 and P8) parieto-occipital regions, as well as the corresponding difference between the two conditions, are presented in Figures 3, 4, 5, 6 and 7, with grey-shaded areas representing significant clusters.

2.7 | Statistical analyses

All statistical analyses were performed with R version 3.4.3. Repeated-measures ANOVAs were conducted with

the package 'afex' version .19–1 with Greenhouse–Geisser correction applied when the assumption of sphericity was violated (Singmann et al., 2015). Pairwise contrasts were used to examine the significant effects further, with Bonferroni adjustment for multiple comparisons. We also calculated Bayes factors to quantify the evidence in favor of the alternative hypothesis over the null hypothesis (BF_{10}), as implemented in the package BayesFactor for R (Morey & Rouder, 2014). Graphics were made with the package ggplot2 (Team, 2013; Wickham, 2016).

3 | RESULTS

3.1 | EEG frequency-domain responses

3.1.1 | Broadband

As seen in Figure 2a, the results indicated significant responses at the group level at the stimulus fundamental frequency (1f = .65 Hz) and the first 13 harmonics in the selected parieto-occipital electrodes (P7, PO7, P5, P3, PO3, O1, Oz, POz, Pz, O2, PO4, P4, P6, PO8 and P8). Prominent responses at these frequencies were visible in the EEG amplitude spectrum of most of the 15 participants. This was confirmed by individual-level significance tests that indicated significant responses at 1f for seven participants and at the first 13 harmonics for 15, 12, 15, 14, 15, 15, 14, 10, 13, 11, 9, 5 and 5 participants, respectively. EEG amplitude at the fundamental frequency and the first 11 harmonics (1f–12f) were kept for further analyses.

A 2 × 3 × 12 repeated-measures ANOVA with the factors Kinematic (Sinus and Rayleigh), Electrode (left, central and right) and Harmonic (fundamental and 1st–11th harmonics) on the amplitude of broadband EEG data indicated a significant main effect of Harmonic, $F(11, 154) = 19.38$, $p < .0001$, $\eta_g^2 = .34$, $BF_{10} > 100$, showing that EEG responses were the largest for 2f and then decreased for higher harmonics (see Figure 2a). The ANOVA also revealed a significant interaction between Electrode and Harmonic, $F(22, 308) = 5.92$, $p < .0001$, $\eta_g^2 = .10$, $BF_{10} > 100$. Pairwise comparisons conducted for each Harmonic level (36 tests in total) with Bonferroni correction indicated significantly larger responses in lateralized parieto-occipital electrodes compared to central occipital electrodes at 1f – $t(312.81) = 4.00$, $p = .003$, $d = .55$ for left, and $t(312.81) = -4.81$, $p = .001$, $d = .72$ for right—and in central occipital electrodes compared to lateralized parieto-occipital electrodes at 2f – $t(312.81) = -5.94$, $p < .001$, $d = 1.06$ for left, and $t(312.81) = 5.71$, $p < .001$, $d = 1.05$ for right. No other statistically significant differences were found (all p values are >.05). Non-significant effects for the ANOVA should be interpreted with caution due to the possible lack of statistical power.

The amplitude differences between the two kinematics averaged across the fundamental frequency and 11 first harmonics (1f–12f) represented in Figure 2b confirm the absence of difference between Rayleigh and Sinus kinematics for the amplitude of broadband EEG responses, $t(14) = 1.39$, $p = .19$, $d = .35$, $BF_{10} = .59$.

The differences of phase for broadband EEG data between the two kinematics averaged across the fundamental frequency and 11 first harmonics (1f–12f), however, revealed a significant negative phase shift (see Figure 2b), showing earlier response during the observation of Rayleigh compared to Sinus kinematics, $t(14) = -21.76$, $p < .0001$, $d = 5.62$, $BF_{10} > 100$.

3.1.2 | Theta, Alpha, Beta and Gamma frequency bands

As seen in Figure 2c, the results indicated group-level significant responses at 2f for Theta [4–8 Hz] (six significant participants over 15), at 1f and 2f for Alpha [8–12 Hz] (eight and seven significant participants over 15, respectively) and at 1f, 2f and 3f for Beta [12–40 Hz] (12, 12 and 3 significant participants over 15, respectively). No significant response at the group level was found for Gamma [40–100 Hz], and three participants over 15 exhibited a significant response at 1f. EEG amplitude at the fundamental frequency and the first two harmonics (1f–3f) were kept for further analyses on Theta, Alpha, Beta and Gamma responses.

Three-way repeated-measures ANOVAs with the factors Kinematic (Sinus and Rayleigh), Electrode (left, central and right) and Harmonic (fundamental and 1st–2nd harmonics) on the amplitude of Theta, Alpha and Beta indicated a significant main effect of Harmonic—$F(2, 28) = 9.47$, $p = .003$, $\eta_g^2 = .07$, $BF_{10} > 100$ for Theta, $F(2, 28) = 7.81$, $p = .005$, $\eta_g^2 = .09$, $BF_{10} > 100$ for Alpha and $F(2, 28) = 8.35$, $p = .002$, $\eta_g^2 = .09$, $BF_{10} > 100$ for Beta (see Figure 2c). The ANOVA also revealed a significant main effect of Electrode—$F(2, 28) = 4.27$, $p = .03$, $\eta_g^2 = .04$, $BF_{10} = 2.45$ for Theta, $F(2, 28) = 4.44$, $p = .03$, $\eta_g^2 = .04$, $BF_{10} = 1.93$ for Alpha and $F(2, 28) = 4.78$, $p = .03$, $\eta_g^2 = .07$, $BF_{10} = 98.10$ for Beta; and a significant interaction between Electrode and Harmonic—$F(4, 56) = 4.04$, $p = .01$, $\eta_g^2 = .06$, $BF_{10} > 100$ for Theta and $F(4, 56) = 3.51$, $p = .04$, $\eta_g^2 = .04$, $BF_{10} > 100$ for Beta. Pairwise comparisons conducted for each Harmonic level (nine tests in total) with Bonferroni correction for Theta and Beta indicated significantly larger Theta response at 2f in

right parieto-occipital electrodes compared to left parieto-occipital electrodes, $t(83.27) = -3.45$, $p = .008$, $d = .76$, and central occipital electrodes, $t(83.27) = -4.28$, $p = .0005$, $d = .91$, and significantly larger Beta response at 1f in right parieto-occipital electrodes compared to central occipital electrodes, $t(65.08) = -4.72$, $p = .0001$, $d = .91$. Pairwise comparisons (three tests in total, with Bonferroni correction) to explore the main effect of Electrode for Alpha also indicated significantly larger response in right parieto-occipital electrodes compared to central occipital electrodes, $t(28) = -2.98$, $p = .02$, $d = .43$ (see Figure 2c). No other significant effects were revealed by the pairwise comparisons and by the ANOVA conducted on Gamma data (all p values are $>.05$). Non-significant effects for the ANOVAs should be interpreted with caution due to the possible lack of statistical power.

These results show that larger EEG responses occurred in right parieto-occipital regions for Theta, Alpha and Beta frequency bands and that there were no differences in amplitude between the two motion kinematics. This is illustrated in Figure 2b, with the amplitude differences between the two kinematics averaged across the fundamental frequency and first two harmonics (1f–3f) for the different frequency bands—$t(14) = .90$, $p = .38$, $d = .23$, $BF_{10} = .37$ for Theta, $t(14) = .59$, $p = .56$, $d = .15$, $BF_{10} = .31$ for Alpha, $t(14) = -.07$, $p = .94$, $d = .02$, $BF_{10} = .26$ for Beta and $t(14) = -.40$, $p = .69$, $d = .10$, $BF_{10} = .28$ for Gamma.

As for broadband EEG data, exploratory analyses on the phase difference between the two kinematics computed from participants that exhibited significant (signal amplitude > noise background) responses within the fundamental frequency and first two harmonics (and averaged across all significant frequency bins and selected parieto-occipital electrodes) revealed a significant negative phase shift for Alpha and Beta—$t(8) = -2.68$, $p = .03$, $d = .89$, $BF_{10} = 2.83$ and $t(13) = -6.44$, $p < .00001$, $d = 1.72$, $BF_{10} > 100$, respectively (see Figure 2b). No statistical analyses were conducted on Theta and Gamma bands due to only a few participants exhibiting significant activity in these frequency bands (i.e., 6 and 3, respectively; see Figure 2b for individual data).

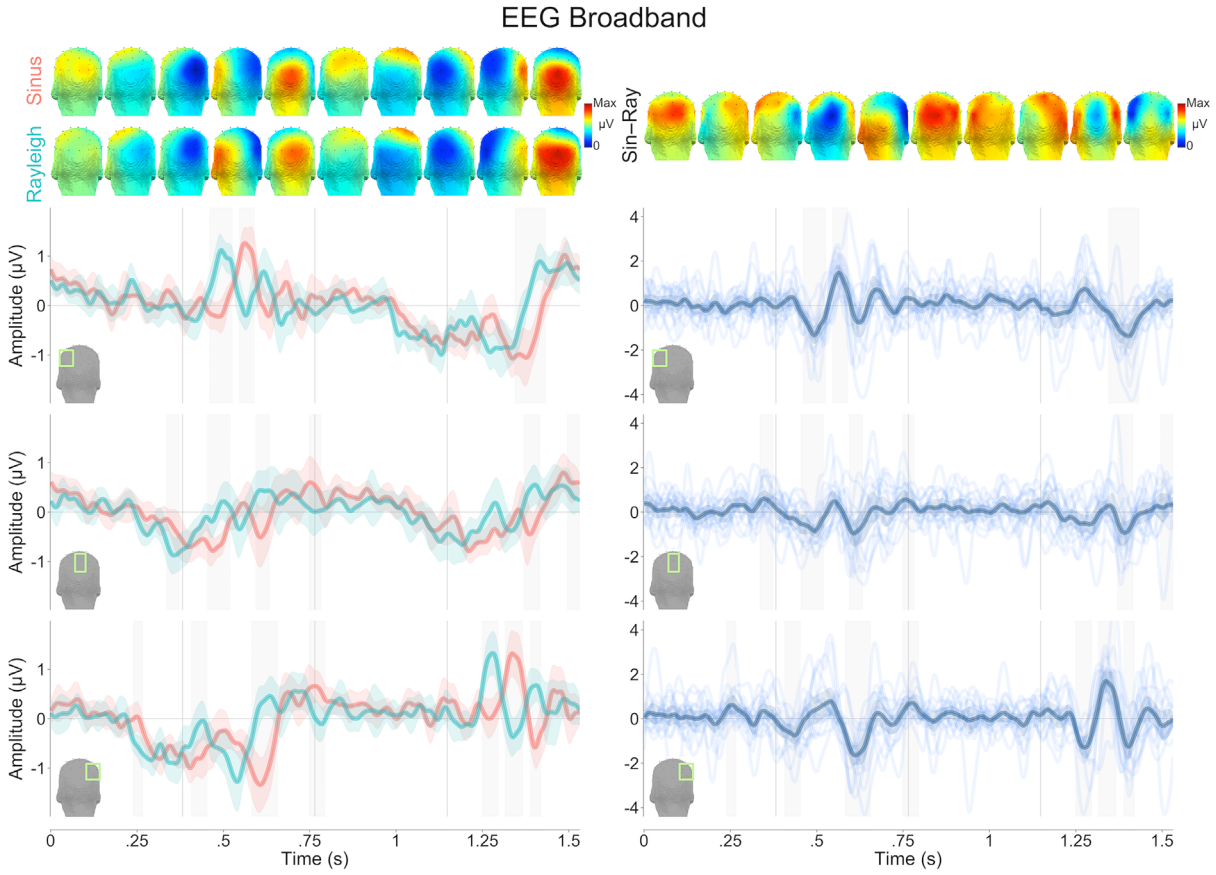

FIGURE 3 Broadband electroencephalography (EEG) time-domain responses for left, central and right selected parieto-occipital electrodes for the two kinematics (and their difference) with the corresponding grand-averaged (posterior view) topographies averaged within 153 ms time windows (1f period/10). Colored shaded areas represent 1 × 95% CI of the mean computed for within-subject designs (Morey, 2008). Grey-shaded areas represent clusters of significant differences between the two kinematics.

3.2 | EEG time-domain responses

3.2.1 | Broadband

As seen in Figure 3, time-domain analyses confirm the absence of difference in amplitude between broadband EEG responses to Rayleigh and Sinus kinematics and the occurrence of a phase shift. In line with the difference between the velocity peaks of the two motion kinematics, peaks in broadband EEG, which were lateralized as a function of the direction of the moving stimulus, occurred earlier with Rayleigh compared to Sinus kinematics. This difference is depicted in Figure 3 with grey-shaded areas showing clusters of significant differences ($p < .05$) between the two time series. It can be noted that the difference between the two EEG responses is about 65 ms, whereas the difference between the stimulus velocity peaks is about 200 ms.

3.2.2 | Theta, Alpha, Beta and Gamma frequency bands

As illustrated in Figures 4–7, time-domain analyses on Theta, Alpha, Beta and Gamma data also confirm the results observed in the frequency-domain. Clear amplitude modulations lateralized as a function of the direction of the moving stimulus were observed for Theta, Alpha and Beta. No clear modulations were found for Gamma. Time-domain responses also confirm the difference of phase between the two stimulus kinematics, with earlier Theta, Alpha and Beta responses observed for Rayleigh compared to Sinus kinematics, as shown by the grey-shaded areas indicating clusters of significant differences in Figures 4–7. Furthermore, time-domain analyses also support the occurrence of larger responses at right parieto-occipital electrodes.

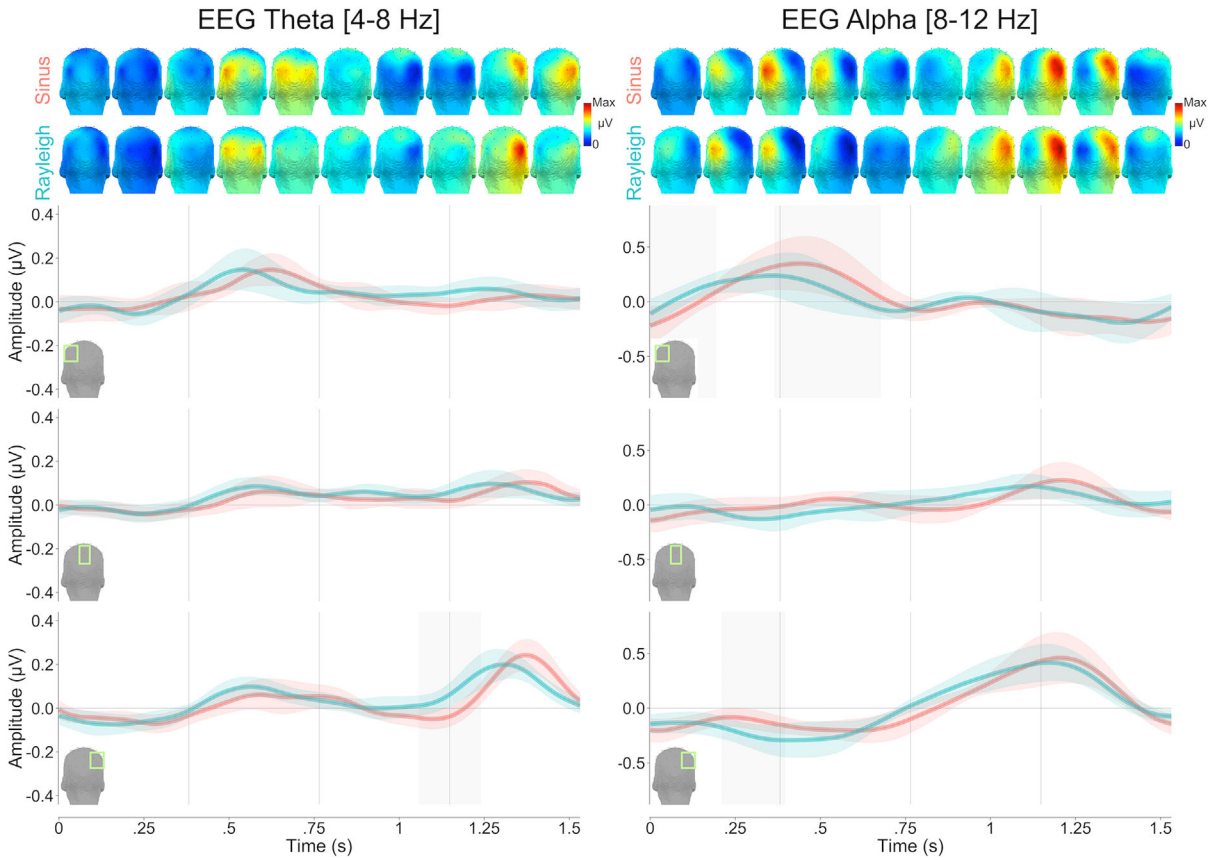

FIGURE 4 Time-domain electroencephalography (EEG) responses in the Theta [4–8 Hz] and Alpha [8–12 Hz] frequency bands for Sinus and Rayleigh kinematics for left, central and right selected parieto-occipital electrodes, with the corresponding grand-averaged (posterior view) topographies averaged within 153 ms time windows (1f period/10). Colored-shaded areas represent 1 × 95% CI of the mean computed for within-subject designs (Morey, 2008). Grey-shaded areas represent clusters of significant differences between the two kinematics.

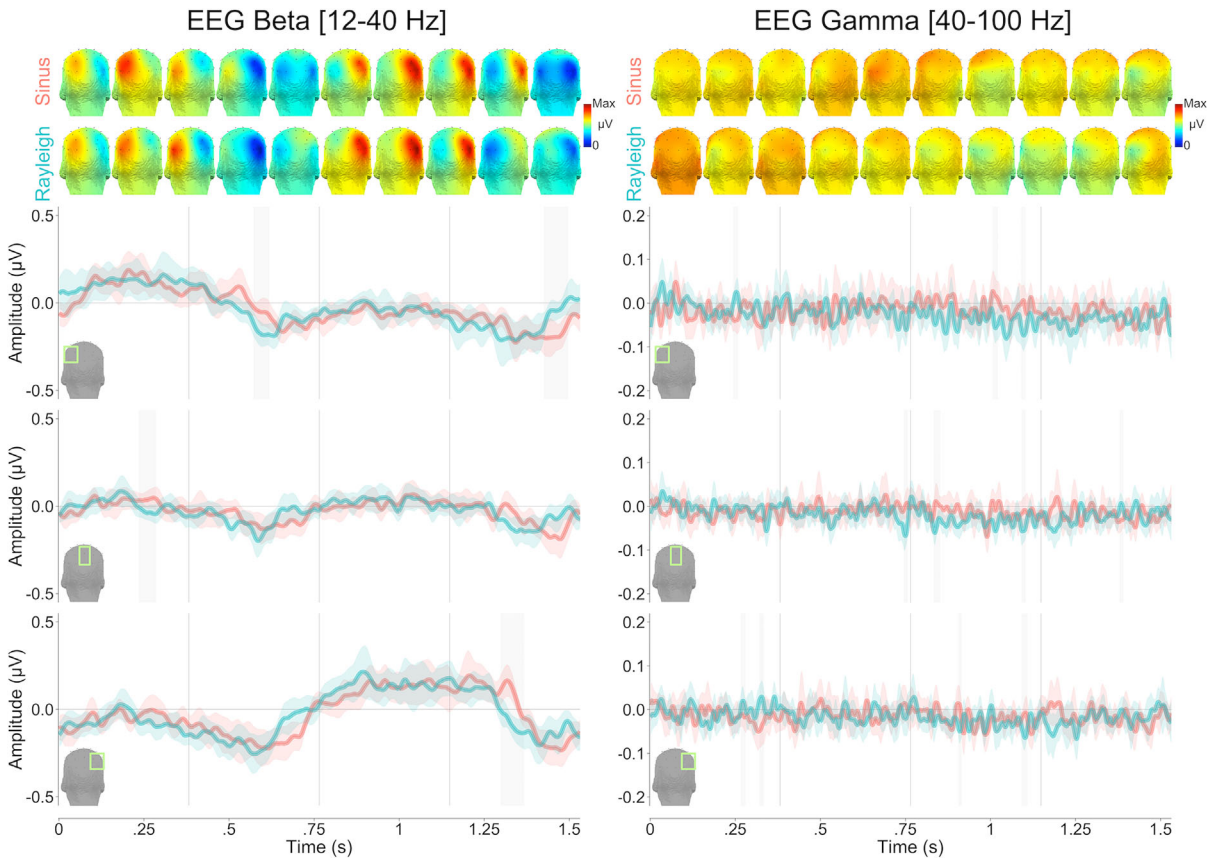

FIGURE 5 Time-domain electroencephalography (EEG) responses in the Beta [12–40 Hz] and Gamma [40–100 Hz] frequency bands for Sinus and Rayleigh kinematics for left, central and right selected parieto-occipital electrodes, with the corresponding grand-averaged (posterior view) topographies averaged within 153 ms time windows (1f period/10). Colored-shaded areas represent 1 × 95% CI of the mean computed for within-subject designs (Morey, 2008). Grey-shaded areas represent clusters of significant differences between the two kinematics.

4 | DISCUSSION

This study investigated how the brain processes visual periodic motion in order to better understand the mechanisms allowing humans to produce precise rhythmic visuomotor synchronization. More specifically, the study examined the relevance of spatiotemporal information contained at the turning points and between turning points of visual periodic motion. We compared EEG responses to sinusoidal oscillations with responses to nonlinear Rayleigh oscillations. Both are typical of human movement and contained the same spatiotemporal information at turning points. However, they contained different spatiotemporal information between the turning points, with Rayleigh oscillations having an earlier peak velocity, which has been shown to increase an individual's capacity to produce accurately synchronized movements. Our results support the relevance of spatiotemporal information (i.e., physical properties) between the turning points, and more specifically of the peak velocity, as indicated by earlier EEG responses to Rayleigh oscillations than sinusoidal oscillations. Our results also suggest that neural oscillations in the Alpha and Beta frequency bands and in the right hemisphere fulfill special functions in the neural tracking of visual periodic movements, as discussed below.

Both frequency-domain and time-domain analyses revealed the effects of spatiotemporal information between the turning points in the neural tracking of visual periodic motion. Different EEG responses to sinusoidal and Rayleigh oscillations occurred despite the two stimuli containing the same spatiotemporal information at turning points. Relatively early EEG peaks in time-domain responses and negative phase shifts in frequency-domain responses were found during the observation of Rayleigh oscillations. This negative phase shift was robustly observed in the EEG broadband signal of all 15 tested participants, as shown in Figure 2b, and by extremely high effect size (Cohen's $d = 5.62$) and Bayes factor ($BF_{10} > 100$). These results extend previous behavioral studies by highlighting the critical role of the velocity peak during the observation of periodic movements at

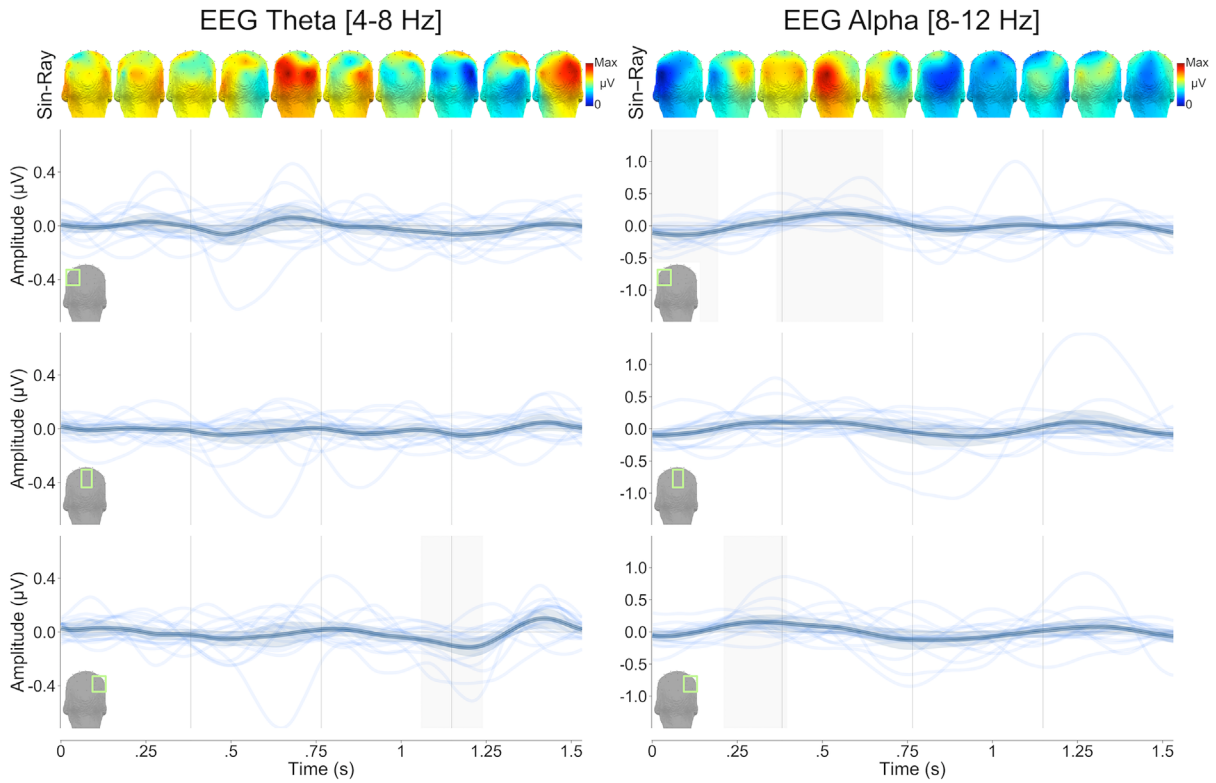

FIGURE 6 Difference between time-domain electroencephalography (EEG) responses in the Theta [4–8 Hz] and Alpha [8–12 Hz] frequency bands for Sinus and Rayleigh kinematics for left, central and right selected parieto-occipital electrodes, with the corresponding grand-averaged (posterior view) topographies averaged within 153 ms time windows (1f period/10). Colored-shaded areas represent 1 × 95% CI of the mean computed for within-subject designs (Morey, 2008). Grey-shaded areas represent clusters of significant differences between the two kinematics.

a neurophysiological level (Gu et al., 2019; Iversen et al., 2015; Kilner et al., 2007; Luck & Toiviainen, 2006; Su, 2016; Varlet et al., 2014). This finding provides a neurophysiological basis for understanding the previously reported enhanced capacity of individuals to synchronize movements with Rayleigh oscillations (Varlet et al., 2014; Varlet, Schmidt, & Richardson, 2017; Zelic et al., 2016). Earlier brain responses enabled by stimulus physical properties, suggesting earlier extraction of functionally relevant timing information, might provide more time for the preparation of an individual's movement and its continuous regulation within stimulus cycles, leading to more precise synchronization. It can be noted that the earlier EEG peak occurring with Rayleigh oscillations is not consistent with the heightened relevance of the acceleration peak in the neural tracking of visual periodic movements, as the acceleration peak for Rayleigh oscillations occurs actually later than the acceleration peak for sinusoidal oscillations (see Figure 1). Nevertheless, the time difference between the peak in the EEG responses to the Sinus and Rayleigh stimuli is shorter than the actual time difference between the peak velocity of the two stimuli, leaving open the possibility that other spatiotemporal information (i.e., physical properties) between the turning points might have contributed to earlier brain responses for Rayleigh oscillations. A broader range of stimuli and velocity peaks would be needed in future studies to confirm the exact role of the velocity peak in visual periodic motion in conveying critical timing information that supports rhythmic visuomotor synchronization. Furthermore, taken alongside the lack of reliable amplitude differences between EEG responses to Rayleigh and Sinus oscillations, these results suggest that the timing of the visual responses in the brain might be more important than their magnitude for enhanced visuomotor synchronization.

Both frequency-domain and time-domain analyses also showed that the brain tracks visual periodic motion and differences in velocity profiles via dynamic amplitude modulations of neural oscillations across different frequency bands. Group-level analyses revealed that large responses in broadband EEG were accompanied by significant responses in Theta (4–8 Hz), Alpha (8–12 Hz) and Beta (12–40 Hz) frequency bands. These responses are clearly visible both in the frequency-domain and time-domain, as seen in Figures 2–7. A few participants

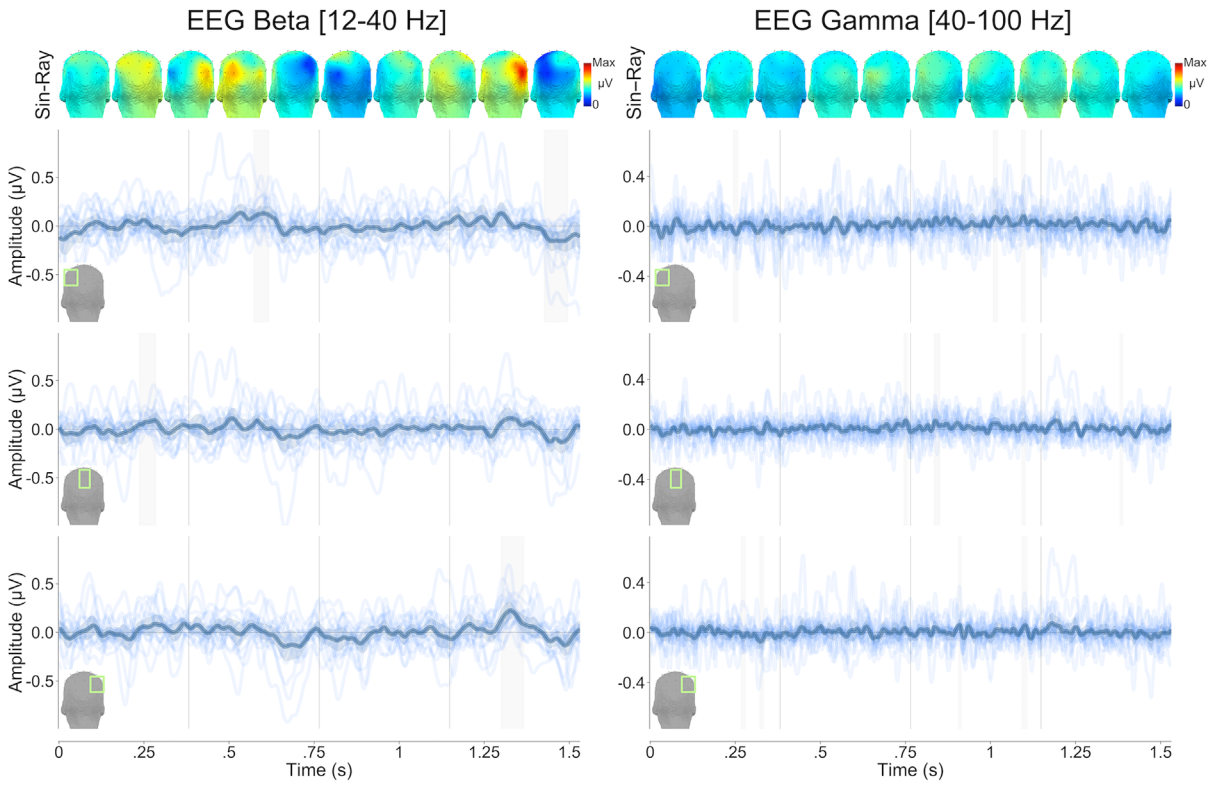

FIGURE 7 Difference between time-domain electroencephalography (EEG) responses in the Beta [12–40 Hz] and Gamma [40–100 Hz] frequency bands for Sinus and Rayleigh kinematics for left, central and right selected parieto-occipital electrodes, with the corresponding grand-averaged (posterior view) topographies averaged within 153 ms time windows (1f period/10). Colored-shaded areas represent 1 × 95% CI of the mean computed for within-subject designs (Morey, 2008). Grey-shaded areas represent clusters of significant differences between the two kinematics.

showed significant responses in the Gamma (40–100 Hz) band, but the involvement of oscillations in this frequency band appears limited although this will need to be further confirmed in future research. It can also be noted that despite the FFT on broadband data showing strong activity in harmonics included in the Theta band, amplitude modulations in Theta oscillations captured by frequency-domain and time-domain analyses on the envelope of 4–8 Hz EEG activity appears relatively small compared to those occurring for the Alpha and Beta bands. Only six out of 15 participants exhibited significant responses in the Theta band, whereas nine and 14 participants exhibited significant responses in the Alpha and Beta bands, respectively. This confirms that the amplitude at higher harmonics in broadband EEG activity does not directly capture amplitude modulations occurring in faster neural oscillations at the stimulus frequency, which are better assessed by frequency-domain analyses conducted on the envelope of the filtered signals.

The involvement of Alpha and Beta bands in sensorimotor and timing processing might explain this difference between frequency bands (Avanzini et al., 2012; Fujioka et al., 2012; Hari et al., 1998; Press et al., 2011). Although caution is needed because of the different numbers of participants with significant responses in the different frequency bands, the negative phase shift observed in broadband EEG was also found to be particularly robust in the Beta band and then the Alpha band compared to the other bands. Large effect size (Cohen's $d = 1.72$) and extremely high Bayes factor ($BF_{10} > 100$) were found for the Beta band. It can also be noted for time-domain responses that although broadband EEG peaks about 200–400 ms after stimulus velocity peaks, this latency seems to decrease with faster neural oscillations. Peaks in the Alpha band are closer to stimulus velocity peaks, and amplitude modulations in the Beta band almost match the stimulus velocity profiles. These results suggest that faster neural oscillations, Beta band neural oscillations in particular (Avanzini et al., 2012; Fujioka et al., 2012; Hari et al., 1998; Press et al., 2011), might play an important role in the neural tracking of visual periodic motion, and more specifically, in the processing of physical properties between the turning points and relevant timing information for visuomotor synchronization.

Furthermore, both frequency-domain and time-domain analyses indicated larger EEG responses to observed periodic movements at right parieto-occipital electrodes compared to left and central parieto-occipital electrodes despite centered stimulus oscillations and participants' gaze fixation. This difference was found in the magnitude of the amplitude modulations of neural oscillations in the Theta, Alpha and Beta frequency bands. These results highlight the role of the right hemisphere in the tracking of periodic movements. We contend that the right–left asymmetry originated from the human-like properties of the kinematics presented in the current study, which would have favored the contribution of brain structures preferentially involved in the perception of biological visual stimuli despite the stimuli being only simple computer-generated red dots. Previous neuroimaging studies have shown a right hemisphere preference for the perception of biological motion and face perception (Grezes et al., 2001; Grossman & Blake, 2001; Hirai et al., 2003; Rossion, 2014). Interestingly, it can be noted that this asymmetry was found in the Theta, Alpha and Beta frequency bands but not in the broadband EEG signal, further supporting the possibility of distinct processes being captured in higher frequency bands. It is nevertheless possible that this asymmetry might be due to an asymmetry in more general attention mechanisms (Śmigasiewicz et al., 2014). Although only one or two letters were presented in each trial, the reading task might also have contributed to this asymmetry. Previous research has shown that reading can result in attention biases towards the reading direction (Mendonça et al., 2020).

Moreover, it can be noted that lateralized responses were observed at the stimulus frequency (1f), whereas centralized responses were observed at its first harmonic (2f), as seen in Figure 2. The most straightforward explanation for these results is that the visual stimulus appeared at left and right turning points at 1f, whereas it appeared at the center at 2f. It is nevertheless possible that these lateralized responses might also reveal more generally the contribution of brain regions specialized in the processing of visual motion, the middle temporal visual area (MT/V5) in particular, which have been shown in both humans and macaque monkeys (Rust et al., 2006; Shipp & Zeki, 1989; Tootell et al., 1995). These open questions encourage further explorations with other stimuli and neuroimaging techniques in order to better understand the hemisphere asymmetry and exact contribution of MT/V5 regions in the neural tracking of visual periodic motion.

Neuroimaging techniques with high temporal and spatial resolutions (e.g., high-density EEG or MEG) would also be advantageous in future studies to further explore the sources and neural network of Beta band activity involved in the tracking of the different velocity profiles. Indeed, although our results show a strong contribution of Beta band neural activity over parieto-occipital regions, Beta activity in other brain regions such as motor regions might also play a critical role, as suggested in previous MEG studies that investigated the neural processing of observed action and periodic events (Fujioka et al., 2012, 2015; Press et al., 2011). Further explorations of the neural activity in the other frequency bands and their role in the processing of visual periodic motion would also be of interest but would require a larger sample size in order to have sufficient statistical power in view of the weaker responses observed in the current study in Theta or Gamma bands at the stimulus frequency.

It will also be important for future research to further investigate the exact nature and function of neural activity in higher frequency bands. Indeed, although distinct dynamics and effects were observed in higher frequency band activity compared to broadband activity, such as in the timing of the amplitude modulations and the hemisphere asymmetry, it remains possible that activity in Theta, Alpha, Beta and Gamma remains largely driven by evoked responses observed in broadband signal. Further research would be needed to determine the exact contribution of dynamic modulations in ongoing neural oscillations rather than in evoked activity in these frequency bands (Busch et al., 2009; Zaehle et al., 2010). Manipulating the predictability of the stimuli is a promising avenue to address this question. Previous research has suggested a critical role of ongoing neural oscillations in predicting and facilitating the processing of periodic stimuli (Friston, 2005; Rimmele et al., 2018). Manipulating the predictability of the Rayleigh and Sinus stimuli used in the current study by occluding some parts of their trajectory and/or adding some frequency variability, for instance, could make it possible to investigate to what extent dynamic changes in higher frequency bands reflect a critical role of ongoing neural oscillations supporting the predictive processing of visual periodic motion.

To conclude, the present study deepens our understanding of how the brain tracks the kinematics of visual periodic motion. It shows the importance of spatiotemporal information contained between the turning points of visual periodic motion and supports the relevance of peak velocity. Our findings indicate that the neural tracking of periodic motions and subtle variations in their velocity profiles involves amplitude modulations of neural oscillations across different frequency bands and parieto-occipital regions. The results suggest a critical role of neural oscillations in the Alpha and Beta bands and of the right hemisphere in the neural tracking of periodic

motion. Together, these findings support at a neurophysiological level the importance of the velocity peak in visual periodic motion in conveying key timing information that allows humans to proficiently synchronize with visual environmental rhythms.

AUTHOR CONTRIBUTIONS

All authors contributed to designing the study, interpreting the results and writing and editing the manuscript. MV collected the data and performed the analyses.

ACKNOWLEDGEMENTS

This work was supported by an Australian Research Council Discovery project (DP170104322). Open access publishing facilitated by Western Sydney University, as part of the Wiley - Western Sydney University agreement via the Council of Australian University Librarians.

CONFLICT OF INTEREST

The authors declare no conflict of interest.

DATA AVAILABILITY STATEMENT

The EEG data, processed data and stimuli used for this study are available on figshare. (https://doi.org/10.6084/m9.figshare.17056916).

ORCID

Manuel Varlet https://orcid.org/0000-0001-5772-2061
Sylvie Nozaradan https://orcid.org/0000-0002-5662-3173

PEER REVIEW

The peer review history for this article is available at https://publons.com/publon/10.1111/ejn.15934.

REFERENCES

Avanzini, P., Fabbri-Destro, M., Dalla Volta, R., Daprati, E., Rizzolatti, G., & Cantalupo, G. (2012). The dynamics of sensorimotor cortical oscillations during the observation of hand movements: An EEG study. *PLoS ONE*, *7*(5), e37534. https://doi.org/10.1371/journal.pone.0037534

Batschelet, E. (1981). *Circular statistics in biology* (Vol. 371). Academic Press London.

Beek, P. J., Schmidt, R. C., Morris, A. W., Sim, M.-Y., & Turvey, M. T. (1995). Linear and nonlinear stiffness and friction in biological rhythmic movements. *Biological Cybernetics*, *73*(6), 499–507. https://doi.org/10.1007/BF00199542

Bingham, G. P. (2004). A perceptually driven dynamical model of bimanual rhythmic movement (and phase perception). *Ecological Psychology*, *16*(1), 45–53. https://doi.org/10.1207/s15326969eco1601_6

Bingham, G. P., Zaal, F. T., Shull, J. A., & Collins, D. R. (2001). The effect of frequency on the visual perception of relative phase and phase variability of two oscillating objects. *Experimental Brain Research*, *136*(4), 543–552. https://doi.org/10.1007/s002210000610

Bourguignon, M., Piitulainen, H., Smeds, E., Zhou, G., Jousmäki, V., & Hari, R. (2017). MEG insight into the spectral dynamics underlying steady isometric muscle contraction. *Journal of Neuroscience*, *37*, 0447–0417. https://doi.org/10.1523/JNEUROSCI.0447-17.2017

Bouvet, C. J., Bardy, B. G., Keller, P. E., Dalla Bella, S., Nozaradan, S., & Varlet, M. (2020). Accent-induced modulation of neural and movement patterns during spontaneous synchronization to auditory rhythms. *Journal of Cognitive Neuroscience*, *32*(12), 2260–2271. https://doi.org/10.1162/jocn_a_01605

Brass, M., Bekkering, H., Wohlschläger, A., & Prinz, W. (2000). Compatibility between observed and executed finger movements: Comparing symbolic, spatial, and imitative cues. *Brain and Cognition*, *44*(2), 124–143. https://doi.org/10.1006/brcg.2000.1225

Busch, N. A., Dubois, J., & VanRullen, R. (2009). The phase of ongoing EEG oscillations predicts visual perception. *Journal of Neuroscience*, *29*(24), 7869–7876. https://doi.org/10.1523/JNEUROSCI.0113-09.2009

Calvo-Merino, B., Glaser, D. E., Grèzes, J., Passingham, R. E., & Haggard, P. (2004). Action observation and acquired motor skills: An FMRI study with expert dancers. *Cerebral Cortex*, *15*(8), 1243–1249. https://doi.org/10.1093/cercor/bhi007

Coey, C. A., Varlet, M., & Richardson, M. J. (2012). Coordination dynamics in a socially situated nervous system. *Frontiers in Human Neuroscience*, *6*, 164. http://www.ncbi.nlm.nih.gov/pmc/articles/PMC3369191/, https://doi.org/10.3389/fnhum.2012.00164

Colon, E., Liberati, G., & Mouraux, A. (2017). EEG frequency tagging using ultra-slow periodic heat stimulation of the skin reveals cortical activity specifically related to C fiber thermonociceptors. *NeuroImage*, *146*, 266–274. https://doi.org/10.1016/j.neuroimage.2016.11.045

Faul, F., Erdfelder, E., Lang, A. G., & Buchner, A. (2007). G* power 3: A flexible statistical power analysis program for the social, behavioral, and biomedical sciences. *Behavior Research Methods*, *39*(2), 175–191. https://doi.org/10.3758/BF03193146

Friston, K. (2005). A theory of cortical responses. *Philosophical Transactions of the Royal Society B: Biological Sciences*, *360*(1456), 815–836. https://doi.org/10.1098/rstb.2005.1622

Fujioka, T., Ross, B., & Trainor, L. J. (2015). Beta-band oscillations represent auditory beat and its metrical hierarchy in perception and imagery. *Journal of Neuroscience*, *35*(45), 15187–15198. https://doi.org/10.1523/JNEUROSCI.2397-15.2015

Fujioka, T., Trainor, L. J., Large, E. W., & Ross, B. (2012). Internalized timing of isochronous sounds is represented in neuromagnetic beta oscillations. *Journal of Neuroscience*, *32*(5), 1791–1802. https://doi.org/10.1523/JNEUROSCI.4107-11.2012

Grezes, J., Fonlupt, P., Bertenthal, B., Delon-Martin, C., Segebarth, C., & Decety, J. (2001). Does perception of biological motion rely on specific brain regions? *NeuroImage*, *13*(5), 775–785. https://doi.org/10.1006/nimg.2000.0740

Grossman, E. D., & Blake, R. (2001). Brain activity evoked by inverted and imagined biological motion. *Vision Research*, *41*(10–11), 1475–1482. https://doi.org/10.1016/S0042-6989(00)00317-5

Gu, L., Huang, Y., & Wu, X. (2019). Advantage of audition over vision in a perceptual timing task but not in a sensorimotor timing task. *Psychological Research*, *84*(7), 2046–2056.

Hajnal, A., Richardson, M. J., Harrison, S. J., & Schmidt, R. C. (2009). Location but not amount of stimulus occlusion influences the stability of visuo-motor coordination. *Experimental Brain Research*, *199*(1), 89–93. https://doi.org/10.1007/s00221-009-1958-3

Hari, R., Forss, N., Avikainen, S., Kirveskari, E., Salenius, S., & Rizzolatti, G. (1998). Activation of human primary motor cortex during action observation: A neuromagnetic study. *Proceedings of the National Academy of Sciences*, *95*(25), 15061–15065. https://doi.org/10.1073/pnas.95.25.15061

Hirai, M., Fukushima, H., & Hiraki, K. (2003). An event-related potentials study of biological motion perception in humans. *Neuroscience Letters*, *344*(1), 41–44. https://doi.org/10.1016/S0304-3940(03)00413-0

Hove, M. J., Fairhurst, M. T., Kotz, S. A., & Keller, P. E. (2013). Synchronizing with auditory and visual rhythms: An fMRI assessment of modality differences and modality appropriateness. *NeuroImage*, *67*, 313–321. https://doi.org/10.1016/j.neuroimage.2012.11.032

Hove, M. J., Spivey, M. J., & Krumhansl, C. L. (2010). Compatibility of motion facilitates visuomotor synchronization. *Journal of Experimental Psychology: Human Perception and Performance*, *36*(6), 1525–1534. https://doi.org/10.1037/a0019059

Iversen, J. R., Patel, A. D., Nicodemus, B., & Emmorey, K. (2015). Synchronization to auditory and visual rhythms in hearing and deaf individuals. *Cognition*, *134*, 232–244. https://doi.org/10.1016/j.cognition.2014.10.018

Jacques, C., Retter, T. L., & Rossion, B. (2016). A single glance at natural face images generate larger and qualitatively different category-selective spatio-temporal signatures than other ecologically-relevant categories in the human brain. *NeuroImage*, *137*, 21–33. https://doi.org/10.1016/j.neuroimage.2016.04.045

Jacques, C., & Rossion, B. (2007). Early electrophysiological responses to multiple face orientations correlate with individual discrimination performance in humans. *NeuroImage*, *36*(3), 863–876. https://doi.org/10.1016/j.neuroimage.2007.04.016

Kelso, J. A. (1995). *Dynamic patterns: The self organization of brain and behaviour*. The MIT Press.

Kilner, J., de Hamilton, A. F. C., & Blakemore, S.-J. (2007). Interference effect of observed human movement on action is due to velocity profile of biological motion. *Social Neuroscience*, *2*(3–4), 158–166. https://doi.org/10.1080/17470910701428190

Kilner, J., Paulignan, Y., & Blakemore, S. J. (2003). An interference effect of observed biological movement on action. *Current Biology*, *13*(6), 522–525. https://doi.org/10.1016/S0960-9822(03)00165-9

Kilner, J. M., Marchant, J. L., & Frith, C. D. (2009). Relationship between activity in human primary motor cortex during action observation and the mirror neuron system. *PLoS ONE*, *4*(3), e4925. https://doi.org/10.1371/journal.pone.0004925

Lenc, T., Keller, P. E., Varlet, M., & Nozaradan, S. (2018). Neural tracking of the musical beat is enhanced by low-frequency sounds. *Proceedings of the National Academy of Sciences*, *115*(32), 8221–8226. https://doi.org/10.1073/pnas.1801421115

Lenc, T., Keller, P. E., Varlet, M., & Nozaradan, S. (2019). Hysteresis in the selective synchronization of brain activity to musical rhythm. *BioRxiv*, 696914.

Luck, G., & Sloboda, J. (2008). Exploring the spatio-temporal properties of simple conducting gestures using a synchronization task. *Music Perception*, *25*(3), 225–239. https://doi.org/10.1525/mp.2008.25.3.225

Luck, G., & Sloboda, J. A. (2009). Spatio-temporal cues for visually mediated synchronization. *Music Perception*, *26*(5), 465–473. https://doi.org/10.1525/mp.2009.26.5.465

Luck, G., & Toiviainen, P. (2006). Ensemble musicians' synchronization with conductors' gestures: An automated feature-extraction analysis. *Music Perception: An Interdisciplinary Journal*, *24*(2), 189–200. https://doi.org/10.1525/mp.2006.24.2.189

MacRitchie, J., Varlet, M., & Keller, P. E. (2017). Embodied expression through entrainment and co-representation in musical ensemble performance. In *The Routledge companion to embodied music interaction* (pp. 150–159). Routledge. https://doi.org/10.4324/9781315621364-17

Mendonça, R., Garrido, M. V., & Semin, G. R. (2020). Asymmetric practices of reading and writing shape visuospatial attention and discrimination. *Scientific Reports*, *10*(1), 1–13, 21100. https://doi.org/10.1038/s41598-020-78080-0

Morey, R. D. (2008). Confidence intervals from normalized data: A correction to Cousineau (2005). *Reason*, *4*(2), 61–64. https://doi.org/10.20982/tqmp.04.2.p061

Morey, R. D., & Rouder, J. N. (2014). BayesFactor: Computation of Bayes factors for common designs. R Package Version 0.9.12-4.2, 9(7).

Mouraux, A., & Iannetti, G. D. (2008). Across-trial averaging of event-related EEG responses and beyond. *Magnetic Resonance Imaging*, *26*(7), 1041–1054. https://doi.org/10.1016/j.mri.2008.01.011

Nozaradan, S., Peretz, I., & Keller, P. E. (2016). Individual differences in rhythmic cortical entrainment correlate with predictive behavior in sensorimotor synchronization. *Scientific Reports*, *6*, 20612. https://doi.org/10.1038/srep20612

Nozaradan, S., Schönwiesner, M., Keller, P. E., Lenc, T., & Lehmann, A. (2018). Neural bases of rhythmic entrainment in humans: Critical transformation between cortical and lower-level representations of auditory rhythm. *European Journal of Neuroscience*, *47*(4), 321–332. https://doi.org/10.1111/ejn.13826

Oostenveld, R., Fries, P., Maris, E., & Schoffelen, J.-M. (2011). FieldTrip: Open source software for advanced analysis of MEG, EEG, and invasive electrophysiological data. *Computational Intelligence and Neuroscience*, *2011*, 1–9, 156869. https://doi.org/10.1155/2011/156869

Pikovsky, A., Rosenblum, M., & Kurths, J. (2003). *Synchronization: A universal concept in nonlinear sciences* (Vol. 12). Cambridge university press.

Press, C., Bird, G., Flach, R., & Heyes, C. (2005). Robotic movement elicits automatic imitation. *Cognitive Brain Research*, *25*(3), 632–640. https://doi.org/10.1016/j.cogbrainres.2005.08.020

Press, C., Cook, J., Blakemore, S.-J., & Kilner, J. (2011). Dynamic modulation of human motor activity when observing actions. *The Journal of Neuroscience*, *31*(8), 2792–2800. https://doi.org/10.1523/JNEUROSCI.1595-10.2011

Quek, G., Nemrodov, D., Rossion, B., & Liu-Shuang, J. (2018). Selective attention to faces in a rapid visual stream: Hemispheric differences in enhancement and suppression of category-selective neural activity. *Journal of Cognitive Neuroscience*, *30*(3), 393–410. https://doi.org/10.1162/jocn_a_01220

Repp, B. H., & Su, Y.-H. (2013). Sensorimotor synchronization: A review of recent research (2006–2012). *Psychonomic Bulletin & Review*, *20*, 1–50. https://doi.org/10.3758/s13423-012-0371-2

Rimmele, J. M., Morillon, B., Poeppel, D., & Arnal, L. H. (2018). Proactive sensing of periodic and aperiodic auditory patterns. *Trends in Cognitive Sciences*, *22*(10), 870–882. https://doi.org/10.1016/j.tics.2018.08.003

Roerdink, M., Ophoff, E. D., Peper, C. L. E., & Beek, P. J. (2008). Visual and musculoskeletal underpinnings of anchoring in rhythmic visuo-motor tracking. *Experimental Brain Research*, *184*(2), 143–156. https://doi.org/10.1007/s00221-007-1085-y

Roerdink, M., Peper, C. E., & Beek, P. J. (2005). Effects of correct and transformed visual feedback on rhythmic visuo-motor tracking: Tracking performance and visual search behavior. *Human Movement Science*, *24*(3), 379–402. https://doi.org/10.1016/j.humov.2005.06.007

Rossion, B. (2014). Understanding face perception by means of human electrophysiology. *Trends in Cognitive Sciences*, *18*(6), 310–318. https://doi.org/10.1016/j.tics.2014.02.013

Rust, N. C., Mante, V., Simoncelli, E. P., & Movshon, J. A. (2006). How MT cells analyze the motion of visual patterns. *Nature Neuroscience*, *9*(11), 1421–1431. https://doi.org/10.1038/nn1786

Schmidt, R. C., & Richardson, M. J. (2008). Dynamics of interpersonal coordination. In *Coordination: Neural, behavioral and social dynamics* (pp. 281–308). Springer. https://doi.org/10.1007/978-3-540-74479-5_14

Schmidt, R. C., Richardson, M. J., Arsenault, C., & Galantucci, B. (2007). Visual tracking and entrainment to an environmental rhythm. *Journal of Experimental Psychology: Human Perception and Performance*, *33*(4), 860–870.

Shipp, S., & Zeki, S. (1989). The organization of connections between areas V5 and V1 in macaque monkey visual cortex. *European Journal of Neuroscience*, *1*(4), 309–332. https://doi.org/10.1111/j.1460-9568.1989.tb00798.x

Singmann, H., Bolker, B., Westfall, J., & Aust, F. (2015). afex: Analysis of factorial experiments. R Package Version 0.*13–145*.

Śmigasiewicz, K., Asanowicz, D., Westphal, N., & Verleger, R. (2014). Bias for the left visual field in rapid serial visual presentation: Effects of additional salient cues suggest a critical role of attention. *Journal of Cognitive Neuroscience*, *27*(2), 266–279. https://doi.org/10.1162/jocn_a_00714

Snapp-Childs, W., Wilson, A. D., & Bingham, G. P. (2011). The stability of rhythmic movement coordination depends on relative speed: The Bingham model supported. *Experimental Brain Research*, *215*(2), 89–100. https://doi.org/10.1007/s00221-011-2874-x

Su, Y.-H. (2016). Sensorimotor synchronization with different metrical levels of point-light dance movements. *Frontiers in Human Neuroscience*, *10*, 186. https://doi.org/10.3389/fnhum.2016.00186

Team, R. C. (2013). R: A language and environment for statistical computing.

Tootell, R. B., Reppas, J. B., Dale, A. M., Look, R. B., Sereno, M. I., Malach, R., Brady, T. J., & Rosen, B. R. (1995). Visual motion aftereffect in human cortical area MT revealed by functional magnetic resonance imaging. *Nature*, *375*(6527), 139–141. https://doi.org/10.1038/375139a0

Varlet, M., Bucci, C., Richardson, M. J., & Schmidt, R. C. (2015). Informational constraints on spontaneous visuomotor entrainment. *Human Movement Science*, *41*, 265–281. https://doi.org/10.1016/j.humov.2015.03.011

Varlet, M., Coey, C. A., Schmidt, R. C., Marin, L., Bardy, B. G., & Richardson, M. J. (2014). Influence of stimulus velocity profile on rhythmic visuomotor coordination. *Journal of Experimental Psychology: Human Perception and Performance*, *40*(5), 1849–1860. https://doi.org/10.1037/a0037417

Varlet, M., Novembre, G., & Keller, P. E. (2017). Dynamical entrainment of corticospinal excitability during rhythmic movement observation: A transcranial magnetic stimulation study. *European Journal of Neuroscience*, *45*(11), 1465–1472. https://doi.org/10.1111/ejn.13581

Varlet, M., Nozaradan, S., Nijhuis, P., & Keller, P. E. (2020). Neural tracking and integration of 'self'and 'other' in improvised interpersonal coordination. *NeuroImage*, *206*, 116303. https://doi.org/10.1016/j.neuroimage.2019.116303

Varlet, M., Schmidt, R. C., & Richardson, M. J. (2017). Influence of stimulus velocity profile on unintentional visuomotor entrainment depends on eye movements. *Experimental Brain Research*, *235*(11), 3279–3286. https://doi.org/10.1007/s00221-017-5055-8

Wickham, H. (2016). *ggplot2: Elegant graphics for data analysis*. Springer.

Wilson, A. D., Collins, D. R., & Bingham, G. P. (2005). Perceptual coupling in rhythmic movement coordination: Stable perception leads to stable action. *Experimental Brain Research*, *164*(4), 517–528. https://doi.org/10.1007/s00221-005-2272-3

Zaehle, T., Lenz, D., Ohl, F. W., & Herrmann, C. S. (2010). Resonance phenomena in the human auditory cortex: Individual resonance frequencies of the cerebral cortex determine electrophysiological responses. *Experimental Brain Research*, *203*(3), 629–635. https://doi.org/10.1007/s00221-010-2265-8

Zelic, G., Varlet, M., Kim, J., & Davis, C. (2016). Influence of pacer continuity on continuous and discontinuous visuo-motor synchronisation. *Acta Psychologica*, *169*, 61–70. https://doi.org/10.1016/j.actpsy.2016.05.008

Zelic, G., Varlet, M., Wishart, J., Kim, J., & Davis, C. (2018). The dual influence of pacer continuity and pacer pattern for visuomotor synchronisation. *Neuroscience Letters*, *683*, 150–159. https://doi.org/10.1016/j.neulet.2018.07.044

How to cite this article: Varlet, M., Nozaradan, S., Schmidt, R. C., & Keller, P. E. (2023). Neural tracking of visual periodic motion. *European Journal of Neuroscience*, *57*(7), 1081–1097. https://doi.org/10.1111/ejn.15934